Original Article

sciendo

# Effects of des-acyl ghrelin on insulin sensitivity and macrophage polarization in adipose tissue

**Fang Yuan[1], Qianqian Zhang[1,2], Haiyan Dong[3], Xinxin Xiang[1,4], Weizhen Zhang[1], Yi Zhang[3], Yin Li[1,2]**

[1]Department of Physiology and Pathophysiology, School of Basic Medical Sciences, Peking University, Beijing 100191, China;
[2]Department of Integration of Chinese and Western Medicine, School of Basic Medical Sciences, Peking University, Beijing 100191, China;
[3]Department of Gynecology, the First Affiliated Hospital of China Medical University, Shenyang 110001, Liaoning Province, China;
[4]Department of Pathology, Central Hospital of Zibo, Zibo 255000, Shandong Province, China

## ABSTRACT

**Background and Objectives**: Obesity is the accumulation of adipose tissue caused by excess energy in the body, accompanied by long-term chronic low-grade inflammation of adipose tissue. More than 50% of interstitial cells in adipose tissue are macrophages, which produce cytokines closely related to insulin resistance. Macrophage biology is driven by two polarization phenotypes, M1 (proinflammatory) and M2 (anti-inflammatory). This study aimed to investigate the effect of gastric hormone des-acyl ghrelin (DAG) on the polarization phenotype of macrophages and elucidate the role of macrophages in adipose tissue inflammation and insulin sensitivity and its molecular mechanism. **Methods**: Mice were subcutaneously administrated with DAG in osmotic minipumps. The mice were fed a normal diet or a high-fat diet (HFD). Different macrophage markers were detected by real-time revere transcription polymerase chain reaction. **Results**: Exogenous administration of DAG significantly inhibited the increase of adipocyte volume caused by HFD and reduced the number of rosette-like structures in adipose tissue. HFD in the control group significantly increased M1 macrophage markers, tumor necrosis factor α (TNFα), and inducible NO synthase (iNOS). However, these increases were reduced or even reversed after DAG administration *in vitro*. The M2 markers, macrophage galactose type C-type Lectin-1 (MGL1), arginase 1 (Arg1), and macrophage mannose receptor 1 (MRC1) were decreased by HFD, and the downward trend was inhibited or reversed after DAG administration. Although Arg1 was elevated after HFD, the fold increase after DAG administration *in vitro* was much greater than that in the control group. **Conclusion:** DAG inhibits adipose tissue inflammation caused by HFD, reduces infiltration of macrophages in adipose tissue, and promotes polarization of macrophages to M2, thus alleviating obesity and improving insulin sensitivity.

**Key words**: des-acyl ghrelin, macrophage polarization, adipose tissue, obesity, insulin sensitivity

**Address for Correspondence:**
Dr. Yin Li, Department of Integration of Chinese and Western Medicine, School of Basic Medical Sciences, Peking University, Beijing 100191, China.
E-mail: yinli@bjmu.edu.cn
Dr. Yi Zhang, Department of Gynecology, the First Affiliated Hospital of China Medical University, Shenyang 110001, Liaoning, China. E-mail: syzi@163.com

**Access this article online**

**Website:** www.intern-med.com

**DOI:** 10.2478/jtim-2021-0025

**Quick Response Code:**

## INTRODUCTION

Ghrelin, an intrinsic ligand for the growth hormone secretory receptor (GHSR), was discovered by Kojima *et al.* in 1999.[1] Ghrelin is a peptide hormone mainly produced in the stomach, with an active form activated by ghrelin O-transferase, and a degradation product. Acyl ghrelin exerts central or peripheral biological functions through the GHSR1a receptor, which regulates mammalian somatic growth, feeding habits, energy balance, and anti-inflammatory effects, and regulates the movement of the stomach and small intestine and the secretion of gastric acid.[1–6] Des-acyl ghrelin (DAG) can antagonize the function of ghrelin in energy balance and gastrointestinal motility, and it can promote proliferation of islet B cells, homing and angiogenesis of endothelial progenitor cells, anabolism of C2C12 cells, and muscle

remodeling. In the metabolism of glycolipids that we are concerned with, it has been reported that DAG can reduce the fat content of rodents, reduce postprandial blood glucose, and improve insulin resistance.[7]

At present, the main starting site of chronic inflammatory reaction is adipose tissue. During the development of obesity, adipocytes secrete inflammatory cytokines, such as tumor necrosis factor α (TNFα) and monocyte chemoattractant protein 1 (MCP1), and recruit macrophages to infiltrate adipose tissue.[8] Subsequently, the inflammatory signaling pathway is intensified by activated adipose tissue macrophages (ATMs),[8,9] which in turn produces insulin resistance. Adipocytes interact with macrophages to form a vicious circle of inflammation.

In recent years, it has been found that macrophages play an important role in chronic inflammation of obese adipose tissue. Macrophage infiltration is observed in adipose tissue of obese patients and obese mouse models.[10–12] ATMs are the major source of inflammatory mediators and are the most important mediators of inflammatory responses under obese conditions.[13,14] Macrophages are broadly classified into classical activation of proinflammatory M1 macrophages, which mainly secretes proinflammatory factors [interleukin (IL)6, IL1β, TNFα, *etc.*] and a chemokine (MCP1), and alternative activation of anti-inflammatory M2 macrophages, which mainly secrete anti-inflammatory factors (IL4, IL10, IL12, *etc.*) and growth factors [insulin-like growth factor 1 (IGF1), vascular endothelial growth factor (VEGF), transforming growth factor (TGF), *etc.*].[15–19] M1 and M2 ATMs constitute different subsets of macrophages. Insulin resistance and adipose tissue inflammation are related to the number of M1 macrophages and the expression of M1 marker genes, such as *Tnfa* and *Mcp1*. Moreover, the ratio of M1 to M2 was increased by high-fat diet (HFD)-induced obesity.[20,21]

The peroxisome proliferator-activated receptors (PPARs) are a subset of the nuclear receptor superfamily. There are three forms of PPAR receptors: α, β/δ, and γ.[22] Previous studies have shown that PPARγ is associated with inflammatory diseases.[23–25] Activation of PPARγ significantly reduces adipocyte volume and inhibits white adipose tissue inflammation and adipocyte hypertrophy.[26,27] Loss of PPARγ in immune cells disrupts the ability of abscisic acid to increase insulin sensitivity by inhibiting MCP1 expression and macrophage immersion into white adipose tissue.[28] Normal skeletal muscle and hepatic insulin sensitivity and thiazolidinediones have sufficient antidiabetic effects, and PPARγ is essential in this process.[29] Moreover, PPARγ activator improves inflammation of atherosclerosis and acts as an anti-inflammatory mediator of human T lymphocytes.[30]

The mammalian target of rapamycin (mTOR) is an intracellular fuel sensor that is critical for cell growth, energy homeostasis, and metabolism.[31,32] mTOR has been reported to promote anabolic processes such as synthesis of proteins, nucleotides, fatty acids, and lipids, as well as angiogenesis and catabolic processes such as autophagy.[33,34] This pathway regulates many major cellular processes and is associated with an increasing number of pathological conditions, including cancer, obesity, type 2 diabetes, and neurodegeneration.[35] In particular, it has been shown that ceramide 1-phosphate stimulates macrophage growth by activating the mTOR/p70S6K pathway, and this process is associated with previous stimulation of the PI3K/PKB pathway.[36]

In this study, we investigated whether DAG can improve adipose tissue inflammation by improving the polarization of M1/M2 macrophages in adipose tissue, thereby improving obesity and increasing insulin sensitivity, and the signaling pathways of this process.

## MATERIALS AND METHODS

### *Materials*

DAG was purchased from Phoenix Pharmaceuticals Inc. (Burlingame, CA, USA). Rabbit phospho-AKT (Ser473), phospho-S6, protein kinase B (AKT), S6, phosphatase and tensin homolog (PTEN), and PPARγ antibodies were purchased from Cell Signaling Technology (Beverly, MA, USA). Rosiglitazone, rapamycin, leucine, rat lysosomal-associated membrane protein 2 (LAMP2, Mac3) antibody, and chicken anti-rabbit fluorescein isothiocyanate-conjugated IgG were purchased from Santa Cruz Biotechnology Inc. (Santa Cruz, CA, USA). DyLigh 594-goat anti-rat IgG was purchased from Abbkine Scientific Co (Wuhan, China).

### *Ethical approval*

The research related to animals use has been complied with all the relevant national regulations and institutional policies for the care and use of animals.

### *Animals and treatments*

C57BL/6J mice and DAG-treated mice were used in this study. Six-week-old male mice were housed in specific pathogen-free microisolators and maintained in a regulated environment (24°C, 12-h light-dark cycle, with lights on at 07:00 am). Regular chow and water were available *ad libitum*. Mice were assigned to receive standard laboratory chow (normal chow diet, NCD) or HFD (45% fat, D12451; Research Diets, New Brunswick, NJ, USA) for 12 weeks.

Surgery and implantation of osmotic minipumps: Mice were anesthetized with isoflurane. A 1-cm incision was made in the back skin, and mice were implanted

subcutaneously with an Alzet osmotic minipump (model 1002) filled with vehicle or DAG (11 nmol/kg/d) for 14 d. Before implantation, pumps were filled with the test agent and then placed in a Petri dish with sterile 0.9% saline (NS) at 37 °C for at least 4 h before implantation to prime the pumps.

### *Cell culture*

RAW264.7 cells, a murine peritoneal macrophage-like cell line, mouse-derived peritoneal macrophages, and bone marrow-derived peritoneal macrophages were cultured in high-glucose Dulbecco's modified Eagle's medium (Invitrogen, Grand Island, NY, USA) supplemented with 10% heat-inactivated fetal bovine serum (Gibco, Grand Island, NY, USA), 100 U/mL penicillin, and 100 U/mL streptomycin (Invitrogen) and incubated at 37°C with 5% $CO_2$. Cells were passaged weekly after trypsin-EDTA detachment. All studies were performed on RAW264.7 cells at passages 20–25. The cells were cultured with lipopolysaccharide (LPS; 10 ng/mL) or DAG ($10^{-8}$ M) to generate classically (M1) or alternatively (M2) polarized cells.

### *Glucose tolerance test*

Blood was drawn from a cut at the tip of the tail at 0, 30, 60, 90, and 120 min, and glucose concentrations were detected immediately with Glucotrend from Roche Diagnostics (Mannheim, Germany).

### *RNA extraction and quantitative real-time reverse transcription polymerase chain reaction (RT-PCR) analysis*

Total RNA was isolated using the TRIzol reagent. RT-PCR was conducted in a 25 μL volume containing 2.5 ng cDNA, 5 mM $MgCl_2$, 0.2 mM dNTPs, 0.2 M each primer, 1.25 U AmpliTaq Polymerase, and 1 μL 800´ diluted SYBR Green I stock using the Mx3000 multiplex quantitative PCR system (Stratagene, La Jolla, CA, USA). The RT-PCR program was as follows: holding 95°C for 7 min, 95°C for 30 s, 60°C for 35 s, and 72°C for 35 s. mRNA expression was quantified using the comparative cross threshold (CT) method. The CT value of the housekeeping gene *Actb* was subtracted from the CT value of the target gene to obtain DCT. The normalized fold changes of detected gene mRNA expression were expressed as $2^{-\Delta\Delta CT}$, where ΔΔCT = ΔCT sample - ΔCT control. RT-PCR was performed in duplicate, and each experiment was repeated 4–5 times. Primers used in this study are shown in Table 1.

### *Western blot analysis*

The gastric fundus was quickly harvested, rinsed thoroughly with PBS, and then homogenized on ice in lysis buffer (50 mM Tris-HCl; 15 mm EGTA; 100 mM NaCl; 0.1% Triton X-100 supplemented with protease inhibitor cocktail, pH 7.5). After centrifugation for 10 min at 4°C, the supernatant was used for Western blot analysis. Protein concentration was measured by Bradford's method. A total of 80 μg protein from each sample was loaded onto SDS-PAGE gels. Proteins were transferred to polyvinylidene fluoride membranes. The membranes were incubated for 1 h at room temperature with 5% fat-free milk in Tris-buffered saline containing Tween 20, followed by incubation overnight at 4°C with the primary antibodies. Specific reaction was detected using IRDye-conjugated second antibody and visualized using the Odyssey infrared imaging system (LI-COR Biosciences, Lincoln, NE, USA).

### *Histology*

Mice were deeply anesthetized using pentobarbital. The epididymal adipose tissue was quickly removed and rinsed thoroughly with PBS. The tissue was fixed in 4% paraformaldehyde, dehydrated, embedded in wax, and sectioned at 6 μm. The diameter of each adipocyte in each field was measured using image analysis software ImageJ (v1.48). For each group, cell sizes of about 450 adipocytes from four mice were measured and plotted as histograms.

### *Immunofluorescence*

Mice were deeply anesthetized using pentobarbital. The same part of adipose tissue was quickly removed and rinsed thoroughly with PBS. The tissue was fixed in 4% paraformaldehyde, dehydrated, embedded in wax, and sectioned at 6 μm. Paraffin-embedded sections were dewaxed, rehydrated, and rinsed in PBS. After boiling for 10 min in 10 mM sodium citrate buffer (pH 6.0), sections were blocked in 1% BSA in PBS for 1 h at room temperature, then incubated overnight at 4°C with Mac-3 antibody alone, and then washed in 1 × PBS/0.1% Tween-20 three times for 5 min each. Tissue sections were incubated at room temperature for 1 h with the following secondary antibodies (Dy Ligh 594-goat anti-rat IgG). Controls included substituting primary antibody with rat IgG. The nuclei were visualized by staining with Hoechst 33258 for 10 min. Photomicrographs were taken under a confocal laser-scanning microscope (Leica, Germany).

### *Statistical analysis*

Data were expressed as mean ± SEM. Data analysis used Graph Pad Prism software (v8.0). One-way analysis of variance, Student-Newman-Keul's test (comparisons between multiple groups), or unpaired Student's *t*-test (between two groups) was used as appropriate. $P < 0.05$ denotes statistical significance.

## RESULTS

### *General indexes of DAG-treated mice*

DAG-treated and wild-type mice were fed with NCD or

**Table 1: List and sequence of primers**

| | Upstream primer (5'-3') | Downstream primer (5'-3') |
|---|---|---|
| *Resistin* | TCCTTGTCCCTGAACTGC | ACGAATGTCCCACGAGC |
| *Adiponectin* | ACCAGTATCAGGAAAAGAATGT | TAGAGAAGAAAGCCAGTAAATG |
| *Il6* | AGTTGTGCAATGGCAATTCTG | GGAAATTGGGGTAGGAAGGAC |
| *Pai1* | CCTCACCAACATCTTGGATGCT | TGCAGTGCCTGTGCTACAGAGA |
| *Mcp1* | ACTGAAGCCAGCTCTCTCTTCCTC | TTCCTTCTTGGGTCAGCACAGAC |
| *Tnfa* | CGTCGTAGCAAACCACCAAG | GAGATAGCAAATCGGCTGACG |
| *iNos* | CCAAGCCCTCACCTACTTCC | CTCTGAGGGCTGACACAAGG |
| *Arg1* | CTCCAAGCCAAAGTCCTTAGAG | AGGAGCTGTCATTAGGGACATC |
| *Mgl1* | TGAGAAAGGCTTTAAGAACTGGG | GACCACCTGTAGTGATGTGGG |
| *Mrc1* | AAACACAGACTGACCCTTCCC | GTTAGTGTACCGCACCCTCC |
| *Mrc2* | AAGAAGAAACCCAACGCTACG | CCTCCAGGCTGTCACGAAA |
| *Pparg* | ATCCAGAAGAAGAACCG | AGGCGTTGTAGATGTGC |
| *Actb* | ATCTGGCACCACACCTTC | AGCCAGGTCCAGACGCA |

HFD, and there was no difference in initial body weight. After 10 weeks of feeding, each diet group was divided into two groups and administrated with DAG or NS. Under HFD, exogenous administration of DAG significantly reduced body weight, food intake, and epididymal fat weight (Figure 1A, B, D), and the fat-to-weight ratio was also significantly lower than that of the NS group (Figure 1C), but the difference in water intake was not significant (Supplementary Figure 1), indicating that *in vitro* administration of DAG can improve the development of obesity caused by HFD.

We then performed a glucose tolerance test to check insulin sensitivity. Wild-type mice fed with HFD showed severe hyperglycemia after glucose administration, and impaired glucose tolerance was significantly improved in DAG-administrated mice (Figure 1G). Insulin-induced AKT phosphorylation (Ser473) was significantly inhibited in wild-type mice fed with HFD, but not in mice with exogenously administered DAG (Figure 1E, F). Therefore, exogenous administration of DAG can improve adipose accumulation and glucose metabolism disorder caused by HFD.

## *Effects of exogenous administration of DAG on adipose tissue in mice*

We then detected the effect of DAG on the morphology of adipose tissue. First, we observed the adipose tissue morphology and interstitial cell infiltration by hematoxylin and eosin (H&E) staining. Exogenous administration of DAG significantly inhibited the increase in cell volume caused by HFD and reduced the number of garland-like structures in the adipose tissue (Figure 2A). Next, we examined the expression and secretion of adipocytokines in adipose tissue. The expression of *adiponectin* (Figure 2B) decreased significantly in mice fed with HFD, while the expression of inflammatory adipokines such as *resistin* (Figure 2C), *Il6* (Figure 2D), and plasminogen activator inhibitor 1 (*Pai1*) (Figure 2E) increased significantly. After exogenous administration of DAG, the changes in cytokines caused by HFD were reversed, indicating that exogenous administration of DAG can improve adipose tissue inflammation caused by HFD.

## *Effect of exogenous administration of DAG on adipose tissue macrophage infiltration and polarization in vivo*

More than 50% of adipose tissue stromal cell infiltration is macrophages, which are sensitive to chemical factors released by adipose tissue under inflammatory conditions and are affected by chemotaxis and aggregation in adipose tissue. We performed immunofluorescence staining of LAMP2 to examine the effects of exogenously administered DAG on macrophage aggregation in adipose tissue and found that exogenously administered DAG reversed the increase in macrophage aggregation caused by HFD (Figure 3A).

The effects of macrophage polarization on its function have been reported. M1 and M2 are two forms of macrophage polarization, which are known as classical activated and alternative activated macrophages, respectively. M1 macrophages are considered to be proinflammatory and promote inflammation, and M2 macrophages are anti-inflammatory and inhibit inflammation. We used real-time RT-PCR to verify the changes in markers of different polarization states of macrophages in epididymal adipose tissue. M1 markers were significantly elevated in macrophages aggregated in the epididymal fat of wild-type mice fed with HFD compared with those fed with NCD (Figure 3B–D), while M2 markers were significantly reduced (Figure 3E–G). However, this phenomenon was reversed by exogenously administered DAG (Figure 3B–G). This indicates that exogenous DAG can effectively inhibit M1 polarization and promote M2 polarization of macrophages in epididymal adipose tissue of mice fed with HFD.

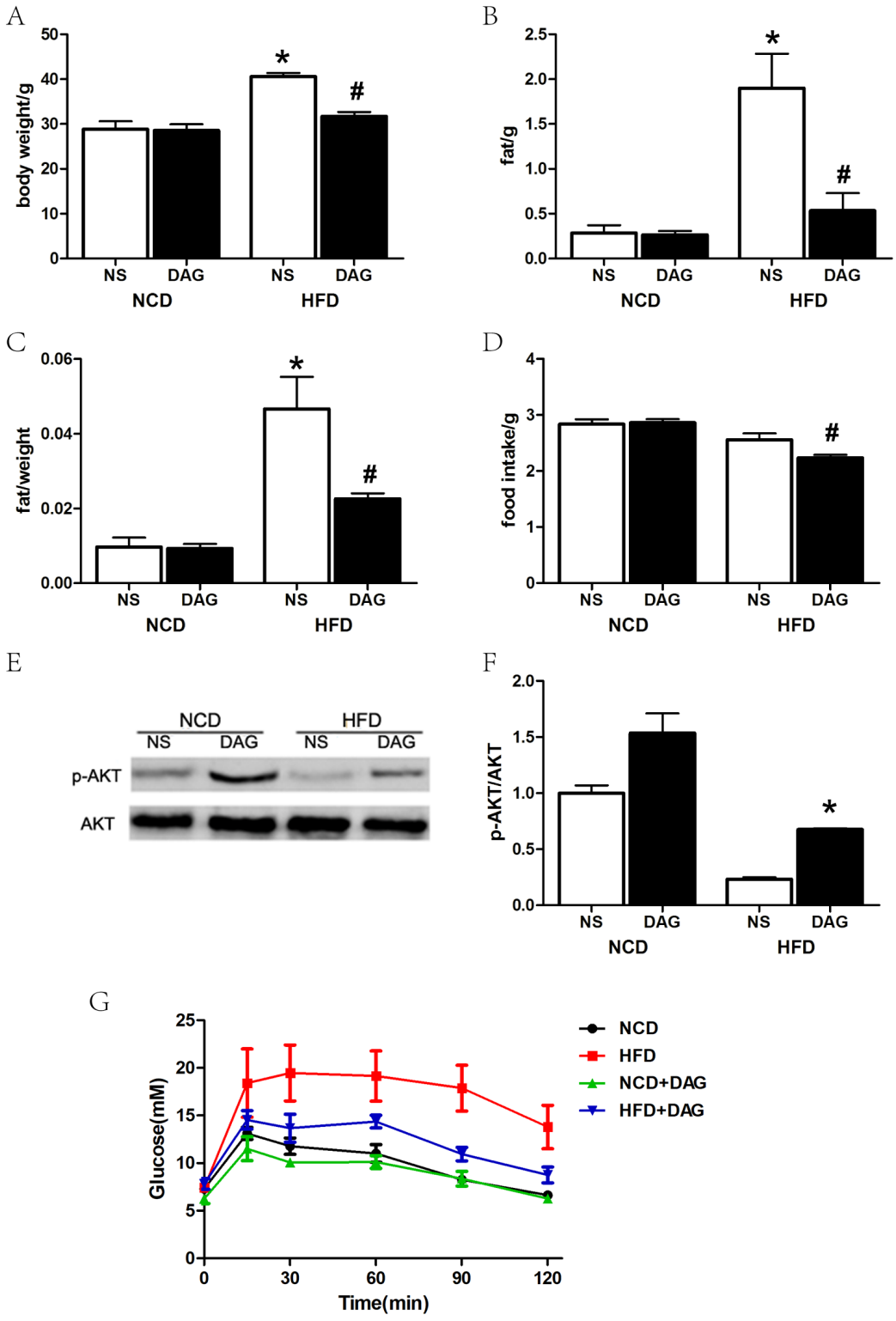


**Figure 1: General indexes of DAG-treated mice. (A) Changes in body weight of DAG- or NS-treated mice fed with NCD or HFD; (B) Weight variation of epididymal adipose tissue in DAG- or NS-treated mice fed with NCD or HFD; (C) Epididymal adipose tissue/body weight ratio of DAG- or NS-treated mice fed with NCD or HFD; (D) Average daily food intake of DAG- or NS-treated mice fed with NCD or HFD; (E) Western blotting results from DAG- and NS-treated mice fed with NCD or HFD. Insulin (2 IU/kg) was injected intraperitoneally 15 min before harvest of adipose tissue, and phospho-AKT (ser473) and AKT in adipose tissue were detected using specific antibodies. Total AKT was used as an internal control; (F) Oral glucose tolerance test using mice with DAG or NS systemically administered by a mini-osmotic pump for 14 days after feeding with NCD or HFD for 10 weeks. All results were expressed as mean ± SEM, $n = 6$. $^{*}P < 0.05$, as compared with NCD-fed mice with same treatment; $^{\#}P < 0.05$, as compared with NS-treated mice fed with same diet. DAG: des-acyl ghrelin; HFD: high-fat diet; NCD: normal chow diet; NS: normal saline.**

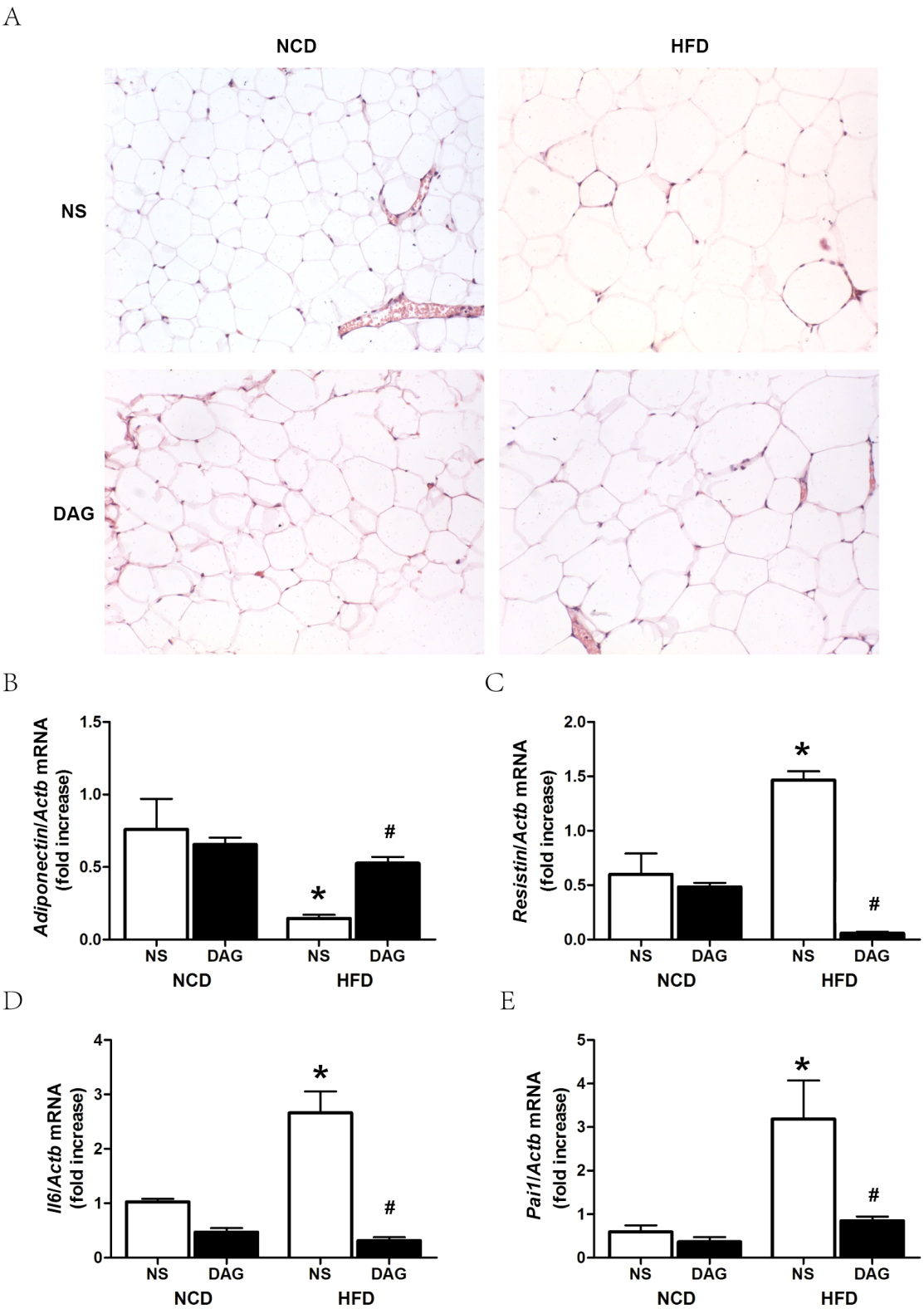


**Figure 2: Adipocyte volume, interstitial cell infiltration, and expression of inflammatory adipokines in epididymal adipose tissue of DAG-treated mice. (A) Epididymal adipose tissues were harvested from C57BL/6 mice with different diets, which were treated with DAG or NS, and processed for H&E staining. mRNAs were extracted from the epididymal adipose tissue harvested from the DAG- and NS-treated mice fed with different diets. Real-time RT-PCR was performed to evaluate mRNA expression of adipokines, such as anti-inflammatory adipokine *adiponectin* (B) and proinflammatory adipokines *resistin* (C), *Il6* (D), and *Pai1* (E). All results were expressed as mean ± SEM, $n = 4$. *$P < 0.05$, as compared with NCD-fed mice with same treatment; #$P < 0.05$, as compared with NS-treated mice fed with same diet. DAG: des-acyl ghrelin; HFD: high-fat diet; NCD: normal chow diet; NS: normal saline.**

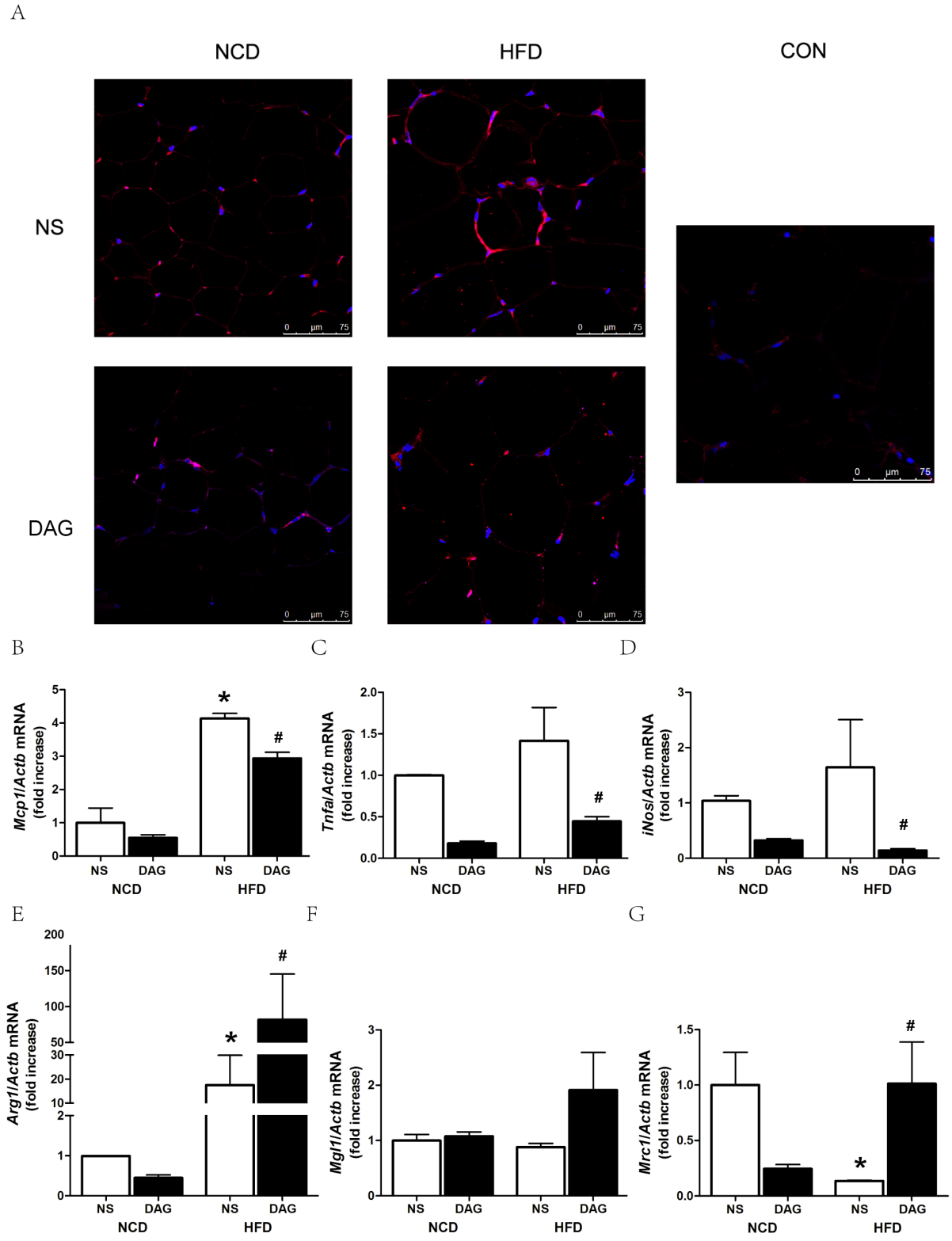


**Figure 3: Effect of DAG systemically administered by a mini-osmotic pump on macrophage infiltration in epididymal adipose tissue. (A) Epididymal adipose tissue was harvested from DAG- and NS-treated mice fed with different diets, and processed for immunofluorescence staining. mRNAs were extracted from the epididymal adipose tissue harvested from the DAG- and NS-treated mice fed with different diets. Real-time RT-PCR was performed to evaluate the expression of macrophage-specific markers. M1 markers *Mcp1* (B), *Tnfa* (C), and *iNos* (D); and M2 markers *Arg1* (E), *Mgl1* (F), and *Mrc1* (G) were detected. All results were expressed as mean ± SEM, $n = 4$. $^{*}P < 0.05$, as compared with NCD-fed mice with same treatment; $^{\#}P < 0.05$, as compared with NS-treated mice fed with same diet. DAG: des-acyl ghrelin; HFD: high-fat diet; NCD: normal chow diet; NS: normal saline; CON: control.**

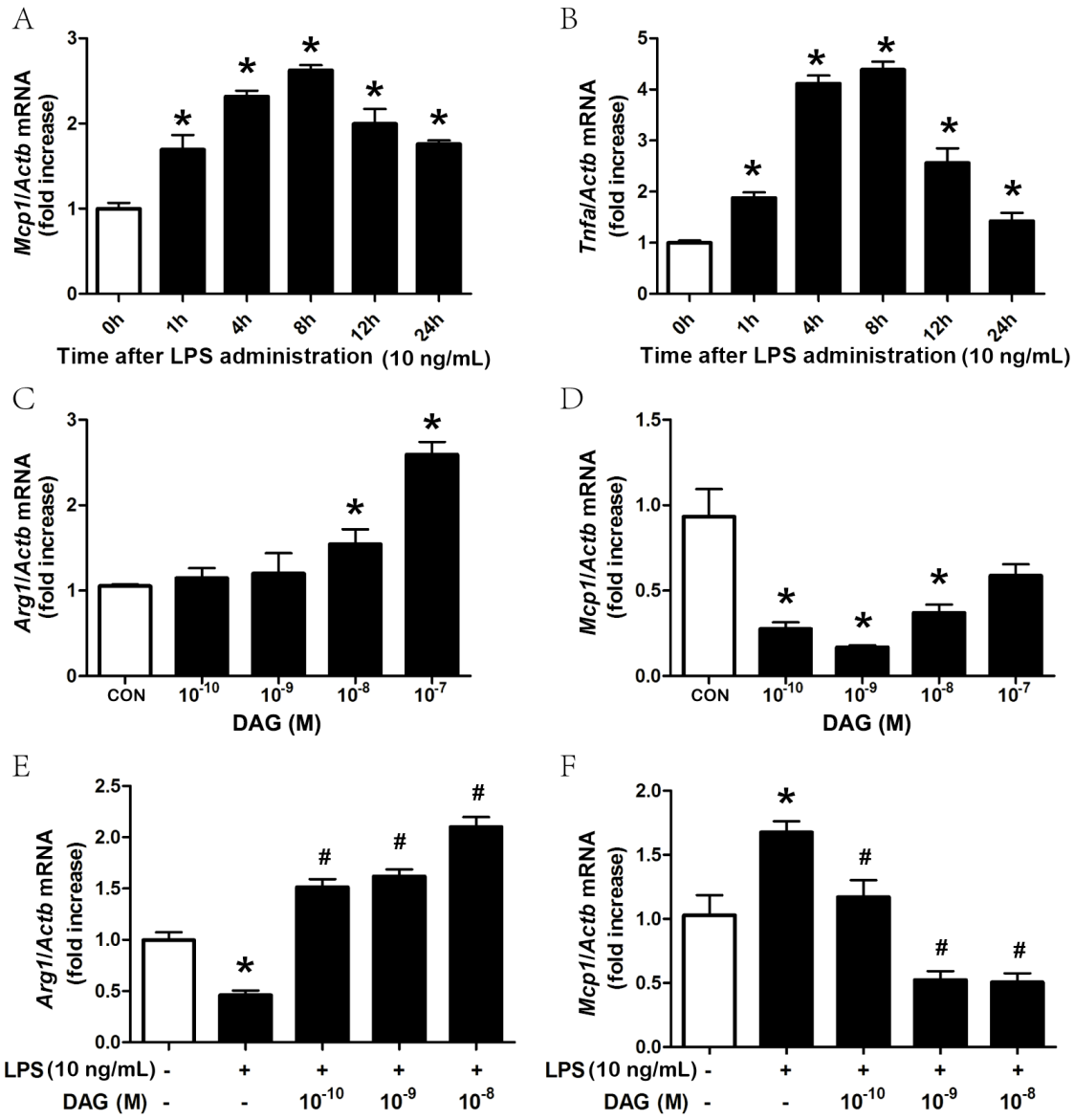


**Figure 4: Effect of DAG on polarization of mouse mononuclear macrophage cell line RAW264.7. mRNAs were extracted from RAW264.7 cells treated with LPS (10 ng/mL) for 0, 1, 4, 8, 12, and 24 h. Real-time RT-PCR was performed to evaluate the expression of inflammatory factors *Mcp1* (A) and *Tnfa* (B). mRNAs were extracted from the RAW264.7 cells treated with DAG for 6 h (0, $10^{-10}$, $10^{-9}$, $10^{-8}$, $10^{-7}$ M). Real-time RT-PCR was performed to evaluate the expression of macrophage-specific markers *Arg1* (C) and *Mcp1* (D). mRNAs were extracted from RAW264.7 cells treated for 30 min with a final concentration of 0, $10^{-10}$, $10^{-9}$, $10^{-8}$ M DAG and then for 6 h with LPS (10 ng/mL). Real-time RT-PCR was performed to evaluate the expression of macrophage-specific markers *Arg1* (E) and *Mcp1* (F). All results were expressed as mean ± SEM, $n = 4$. *$P < 0.05$, as compared with control; #$P < 0.05$, as compared with LPS-treatment alone. DAG: des-acyl ghrelin; CON: control; LPS: lipopolysaccharide; RT-PCR: reverse transcription-polymerase chain reaction.**

## *Effect of DAG on polarization of macrophages in vitro*

We first used mouse mononuclear macrophage cell line RAW264.7 cells to verify whether DAG plays a role in macrophage polarization. As a proinflammatory factor, lipopolysaccharide (LPS) can stimulate the inflammatory response of RAW264.7 cells, which is polarized to the direction of M1. The expression of M1 macrophage-associated markers *Mcp1* and *Tnfa* was significantly induced under 10 ng/ml LPS treatment, with the highest expression at 4–8 h (Figure 4A, B). On the contrary, DAG administration inhibited the expression of *Mcp1* (Figure 4D), but induced the expression of *Arg1* (Figure 4C). To verify whether DAG had a protective effect on inflammatory changes caused by LPS, we treated RAW264.7 cells with LPS (10 ng/mL) and DAG (0, $10^{-10}$, $10^{-9}$, $10^{-8}$ M) together. The decrease in M2 marker expression caused by LPS (Figure 4E) and the increase in M1 marker (Figure 4F)

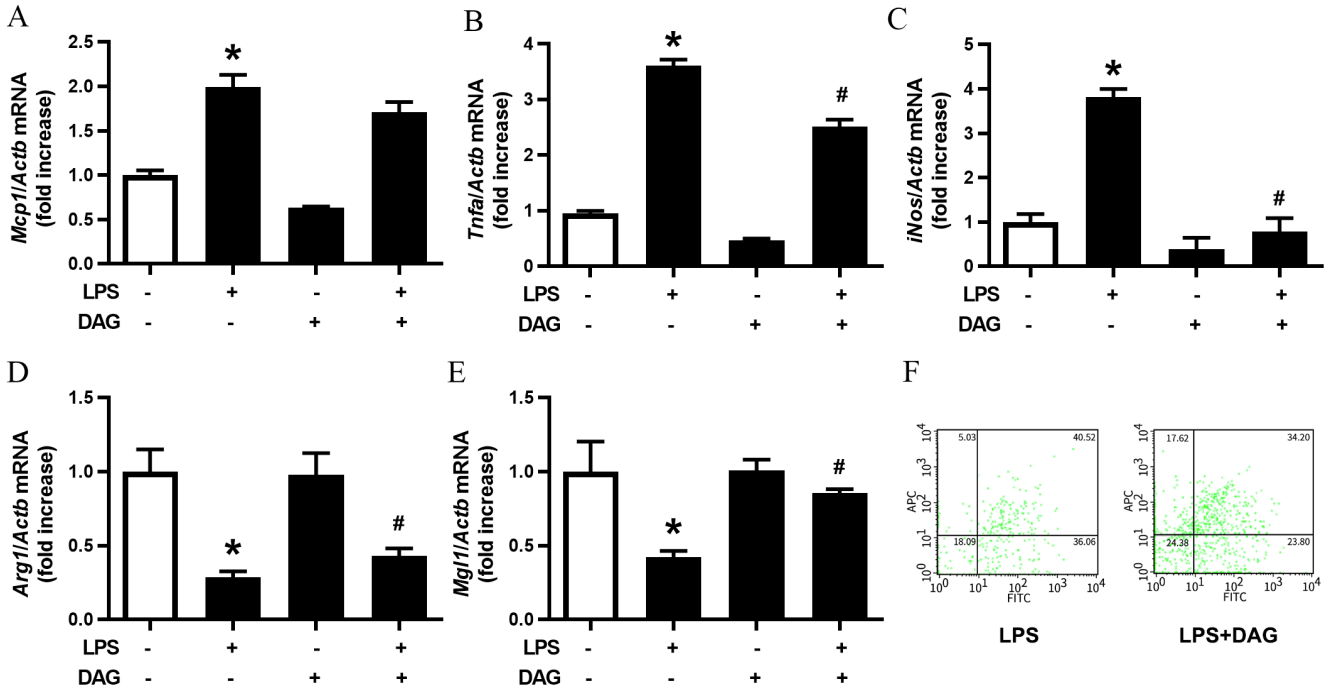


**Figure 5: Effect of DAG on polarization of peritoneal macrophages. mRNAs were extracted from the peritoneal macrophages harvested from wild-type mice fed with NCD. Real-time RT-PCR was performed to evaluate the expression of macrophage-specific markers. M1 markers *Mcp1* (A), *Tnfa* (B), and *iNos* (C) and M2 markers *Arg1* (D) and *Mgl1* (E). All results were expressed as mean ± SEM, $n = 4$. $^{*}P < 0.05$, as compared with control, $^{\#}P < 0.05$, as compared with LPS-treatment alone. F4/80 (PE), CD11c (FITC), and CD206 (Alexa fluor 647) were detected by flow cytometry after treatment with LPS with or without DAG (F). DAG: des-acyl ghrelin; LPS: lipopolysaccharide.**

were all reversed by DAG. The above experiments indicated that DAG inhibits polarization to the M1 phenotype in the inflammatory state and promotes polarization to the M2 phenotype in the mouse mononuclear macrophage cell line RAW264.7 cells.

We then confirmed the above results in mouse peritoneal macrophages. We found that LPS treatment induced the expression of M1 macrophage markers (Figure 5A–C) and inhibited the expression of M2 macrophage markers (Figure 5D, E). Although DAG alone did not significantly alter the expression of the relevant markers, when interacted with LPS, DAG significantly reversed expression changes of inflammation-related markers altered by LPS (Figure 5A–E). For the result of flow cytometry, phycoerythrin (PE)-labeled F4/80 was selected as the total marker for macrophages, fluorescein-isothiocyanate (FITC)-labeled CD11c and Alexa fluor 647-labeled CD206 as markers for M1 and M2, respectively. The reversal effect of DAG on LPS was more obvious. After interaction of DAG and LPS, the number of cells expressing CD11c decreased significantly in the cell population expressing F4/80, while CD206 increased significantly (Figure 5F). These results suggested that DAG can reverse the LPS-induced M1 polarization of macrophages.

Macrophages in peripheral tissues are derived from monocytes in the blood, which in turn are derived from precursor cells in the bone marrow. Bone marrow-derived macrophages (BMDMs) have no obvious tendency to be polarized. Polarization occurs when stimulated by relevant cytokines or chemicals. For example, LPS stimulates conversion to M1, and IL4 stimulates conversion to M2. The above results demonstrated that exogenous administration of DAG can alter the phenotype of macrophages in peripheral tissues. We explored the effect of DAG on macrophage polarization in BMDMs. According to reports in the literature, BMDMs can be transformed into macrophages after 7 days of stimulation by macrophage colony-stimulating factor (10 ng/mL). We took the BM of the limbs of C57BL/6 mice and induced macrophage differentiation for 7 days. LPS administration significantly inhibited the expression of M2 markers (Supplementary Figure 2A) and increased the expression of M1 markers (Supplementary Figure 2B); DAG significantly reversed the effect of LPS on different markers of macrophages.

The above experiments confirmed that DAG can affect polarization of mouse peritoneal macrophages, primary BMDMs, and mouse monocyte macrophage cell lines, inhibit macrophage M1 polarization in the inflammatory state, and promote the polarization to the M2 phenotype.

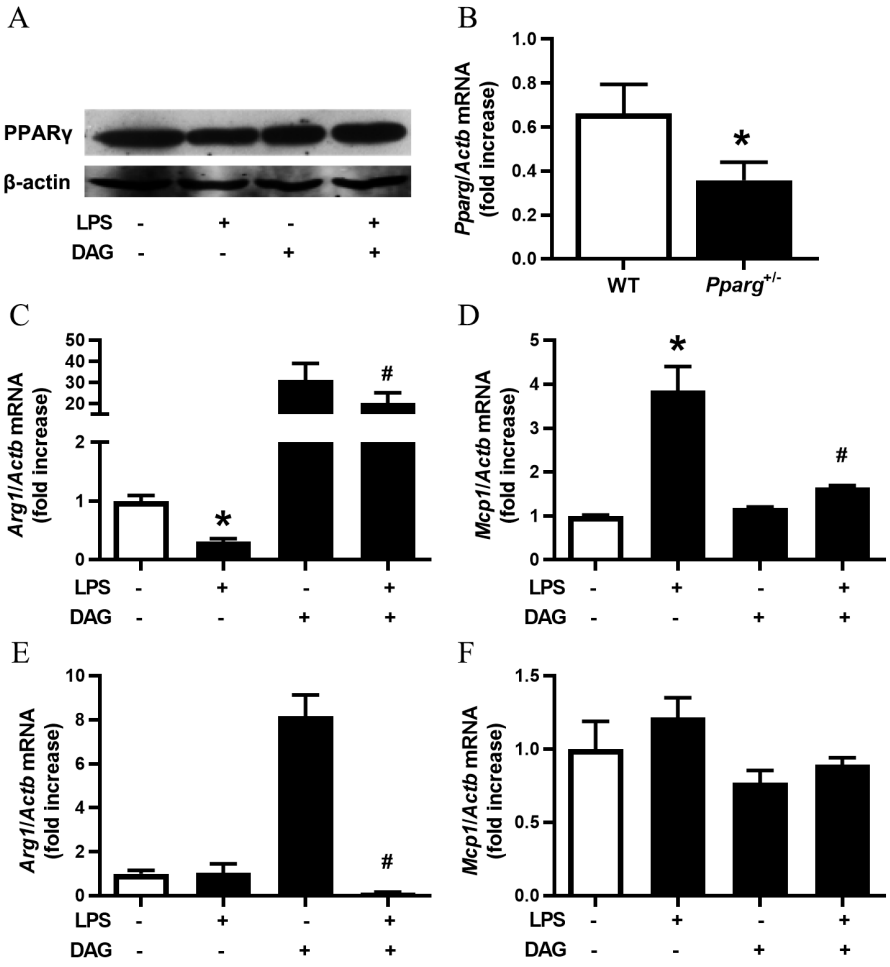


**Figure 6: Direct effect of DAG on polarization of BMDMs isolated from *Pparg*$^{+/-}$ mice. (A) RAW264.7 cells were treated with LPS and/or DAG. Protein level of PPARγ was detected by Western blotting, and β-actin was used as an internal control. (B) Confirmation of *Pparg* expression in *Pparg*$^{+/-}$ and wild-type (WT) mice, **P* < 0.05, as compared with WT mice. BMDMs isolated from WT mice (C, D) and *Pparg*$^{+/-}$ mice (E, F) were treated with NS or LPS (10 ng/mL), with or without DAG (10$^{-8}$ M). mRNAs were extracted, and real-time RT-PCR was performed to evaluate the expression of macrophage-specific markers. M2 marker *Arg1* (C, E) and M1 marker *MCP1* (D, F) were detected. All results were expressed as mean ± SEM, *n* = 4. **P* < 0.05, as compared with control; #*P* < 0.05, as compared with LPS-treatment alone. DAG: des-acyl ghrelin; LPS: lipopolysaccharide.**

## *DAG may inhibit inflammation by activating PPARγ*

PPARγ may be involved in the polarization of macrophages. LPS inhibited the protein level of PPARγ, while DAG reversed the inhibition effect of LPS (Figure 6A) in RAW264.7 cells. We treated RAW264.7 cells with LPS (10 ng/ml) and rosiglitazone (4 μM), the agonist of PPARγ, and found that rosiglitazone reversed the LPS-induced upregulation of *Mcp1*, the M1 polarization marker, and the downregulation of *Arg1*, the M2 polarization marker (Supplementary Figure 3).

To verify whether PPARγ was involved in the protective effect of DAG, we isolated and cultured BMDMs from *Pparg*$^{+/-}$ mice (*Pparg*$^{-/-}$ mice were embryonic lethal) and control wild-type (WT) mice to induce differentiation into macrophages, and then treated with LPS or DAG. The lower expression of *Pparg* was confirmed in *Pparg*$^{+/-}$ mice (Figure 6B). In WT mice, DAG significantly reversed the LPS-induced upregulation of *Mcp1*, the M1 polarization marker, and the down-regulation of *Arg1*, the M2 polarization marker (Figure 6C, D), whereas in *Pparg*$^{+/-}$ mice, this reversal was obviously weakened (Figure 6E, F).

The above experiments indicate that DAG activates PPARγ, thereby inhibiting the polarization of macrophage to M1 phenotype in the inflammatory state and promoting its polarization to M2 phenotype.

## *DAG inhibits inflammation by inhibiting LPS-activated mTOR signaling pathway*

mTOR is a highly conserved central regulatory molecule of signal integration that regulates cell growth, cell cycle, and cell differentiation, with phosphorylation as

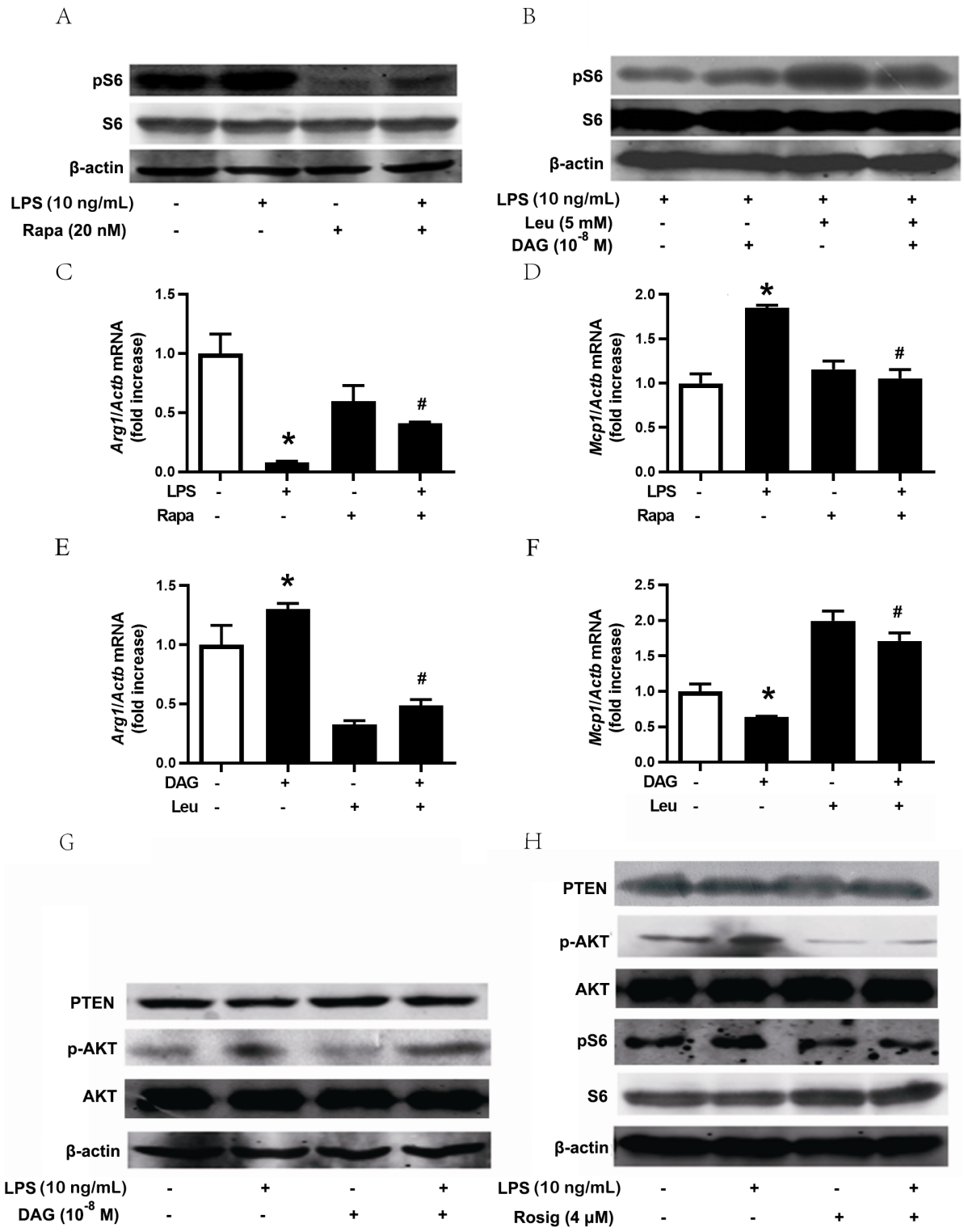


**Figure 7: Role of mTOR signaling pathway in polarization of RAW264.7 cells. (A) Blockade of LPS-induced activation of mTOR and its downstream molecule S6 by rapamycin (Rapa). mRNAs were extracted from RAW264.7 cells treated with rapamycin (20 nM) and then for 6 h with LPS (10 ng/ml). Real-time RT-PCR was performed to evaluate the expression of macrophage-specific markers *Arg1* (C) and *MCP1* (D). All results were expressed as mean ± SEM, $n = 4$. $^{*}P < 0.05$, as compared with control, $^{\#}P < 0.05$, as compared with LPS-treatment alone. (B) Activation of mTOR and its downstream molecule S6 by leucine (Leu, 5 mM). mRNAs were extracted from the LPS-treated RAW264.7 cells with or without DAG or leucine. Real-time RT-PCR was performed to evaluate the expression of macrophage-specific markers *Arg1* (E) and *MCP1* (F). All results were expressed as mean ± SEM, $n = 4$. $^{*}P < 0.05$, as compared with control; $^{\#}P < 0.05$, as compared with DAG-treatment alone. (G) Attenuation of the effect of LPS on PTEN and AKT activation by des-acyl ghrelin in RAW264.7 cells. (H) Attenuation of the effect of LPS on PTEN, AKT, and S6 activation by rosiglitazone in RAW264.7 cells. DAG: des-acyl ghrelin; LPS: lipopolysaccharide; RT-PCR: reverse transcription-polymerase chain reaction.**

activated form. LPS (10 ng/mL) significantly activated the phosphorylation of ribosomal protein S6, the downstream target protein of mTOR in RAW264.7 cells (Figure 7A, Supplementary Figure 4), whereas rapamycin (Figure 7A) and DAG (Supplementary Figure 4) significantly inhibited LPS-induced phosphorylation of S6. The LPS-induced decrease in M2 marker and increase in M1 marker were reversed by rapamycin (Figure 7C, D). On contrary, leucine, the branched chain amino acid used as mTOR signaling activator, blocked the effect of DAG on LPS-induced S6 phosphorylation (Figure 7B). The antagonistic effect of DAG on LPS-regulated macrophage polarization was reversed by leucine (Figure 7E, F). The above experiments indicate that DAG inhibits activation of the mTOR signaling pathway by LPS, thereby inhibiting M1 polarization of macrophages in the inflammatory state and promoting M2 polarization.

A variety of factors can regulate mTOR and its downstream signaling pathways. Among them, the tuberous sclerosis complex (TSC1 and TSC2) can form a stable heterodimeric functional complex, which plays a negative role in the regulation of mTOR activity. The PI3K/AKT signaling pathway activates mTOR and its downstream signaling pathway by inhibiting TSC1 and TSC2. The target gene of PPARγ, the phosphatase and tensin homologue deleted chromatosome 10 (PTEN)-encoded protein, has lipid phosphatase activity and specifically promotes phosphatidylinositol-3,4,5-triphosphate (PIP3) dephosphorylation, thereby inhibiting the PI3K/AKT signal transduction pathway.

We next studied the regulation between PPARγ and mTOR signaling pathway. We found that LPS inhibited PTEN protein in RAW264.7 cells, thereby activating AKT phosphorylation, whereas DAG antagonized the effects of LPS (Figure 7G). The PPARγ agonist rosiglitazone also reversed the inhibition of PTEN and the activation of AKT and S6 caused by LPS (Figure 7H).

## DISCUSSION

This study combined *in vivo* animal models of des-acyl ghrelinemia and cultured cells *in vitro*, using adipose tissue and macrophages as the targets to comprehensively explore the mechanisms of anti-inflammatory and insulin-sensitivity-increasing effects of DAG. Our research showed that exogenous administration of DAG reduced adipose tissue inflammation and macrophage infiltration in adipose tissue, promoted the expression of anti-inflammatory factors in adipose tissue, and inhibited the expression of proinflammatory factors. DAG promoted the expression of M2 markers in anti-inflammatory macrophages and the expression of M1 markers in proinflammatory macrophages through the PPARγ/PTEN/AKT/mTOR signaling pathway, thereby increasing insulin sensitivity in adipose tissue, relieving insulin resistance, and exerting its anti-inflammatory effect.

Insulin resistance is a low-grade chronic inflammatory state,[37] and research on insulin resistance induced by endotoxins through the immune response has confirmed that inflammation and insulin resistance are closely linked.[38,39] Nevertheless, DAG has been shown to have many biological effects, including regulating the differentiation and function of adipocytes, reducing adipose tissue inflammation, inhibiting skeletal muscle atrophy, promoting glucose uptake, and stimulating osteoblast proliferation.[40,41] There are also reports about the direct relationship between DAG and insulin resistance, and human studies have shown that DAG can improve insulin resistance.[7,40–43] Our results show that insulin resistance caused by HFD can be improved by hyper-des-acyl ghrelinemia caused by exogenous administration.

DAG has been reported to be related to macrophage phenotype, but there are few relevant studies. Our research confirmed that DAG can change the polarization trend of macrophages in an inflammatory state. In our mouse model of DAG administered with an exogenous subcutaneous pump, the accumulation of M1 macrophages in adipose tissue caused by HFD was alleviated by DAG. In addition, the main polarizing phenotype of macrophages changed from M1 to M2, suggesting that DAG can increase the sensitivity of insulin in adipose tissue by changing the polarization of macrophages, thereby alleviating insulin resistance and exerting its anti-inflammatory effect.

No studies on mTOR and DAG have been reported. Our study for the first time clarified that LPS can activate mTOR and its downstream target molecule S6. After rapamycin was used to inhibit mTOR signaling, the polarizing effect of LPS on macrophages toward M1 significantly weakened. In addition, DAG can promote the M2 polarization of macrophages by inhibiting the mTOR signaling pathway.

Macrophage M1/M2 polarization can be reversed *in vitro* and *in vivo*.[44] Previous studies have revealed that lipid-induced macrophage M1/M2 polarization can be regulated by directly regulating PPARγ activity.[45] In our study, LPS inhibited the expression of PPARγ, but on this basis, giving DAG can reverse the inhibitory effect of LPS on PPARγ. When rosiglitazone was administered, PPARγ was activated, and the expression of M1 markers was suppressed, while the expression of M2 markers increased. PPARγ agonists are reported to activate PTEN homologs with loss of protein expression on chromosome 10.[46] PTEN is a tumor suppressor protein that inhibits the activation of the

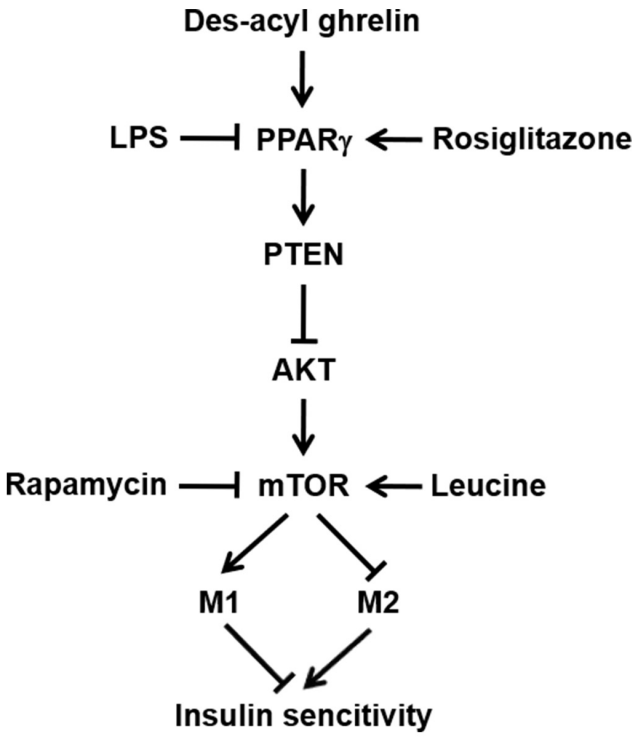


**Figure 8: Illustration of putative signaling pathways. Des-acyl ghrelin improves adipose insulin sensitivity at least partially through modulating the polarization of macrophages via PPARγ/PTEN/AKT/mTOR signaling pathway.**

PI3K/Akt cascade by dephosphorylation of PIP3, thereby generating phosphatidylinositol 4,5-bisphosphate (PIP2). In addition, PI3K/AKT signaling can activate mTOR and its downstream signaling pathways by inhibiting TSC1 and TSC2.[47] We found that LPS inhibited the expression of PTEN protein, thereby activating AKT phosphorylation, promoting phosphorylation of mTOR and downstream molecules and polarization of macrophages toward M1. DAG can antagonize the effect of LPS and reverse the inhibition of PTEN and activation of AKT and mTOR caused by LPS, thereby inhibiting macrophages from polarizing toward M1 and promoting macrophages polarizing toward M2. We therefore concluded that PPARγ/PTEN/AKT/mTOR signaling may be the main pathway for DAG to regulate macrophage polarization.

In summary, this study found that DAG can promote the expression of anti-inflammatory macrophage M2 markers and inhibit the expression of proinflammatory macrophage M1 markers in adipose tissue through the PPARγ/PTEN/AKT/mTOR signaling pathway, which in turn exerts its anti-inflammatory effect and improves insulin sensitivity. The results of this research will help further explore the role of inflammatory immune mechanisms in the development of insulin resistance, and provide new approaches for early prevention and relief of the development of insulin resistance and future screening of drugs that interfere with insulin sensitivity.

## Acknowledgements

We appreciate Professor Jing-Yan Han of Peking University for kindly supporting.

## Source of Funding

This work was supported by the National Natural Science Foundation of China (81873568, 81670780); the National Key Research and Development Program of China (2020YFA0803801); Special project for central guidance of local science and technology development of Liaoning Province (2019JH6/10400006).

## Conflict of Interests

The manuscript has been read and approved by all the authors. The authors declare no conflict of interest.

## Author contributions

Fang Yuan, Qianqian Zhang, Haiyan Dong, and Xinxin Xiang: experimental studies, data acquisition, manuscript preparation; Weizhen Zhang, Yi Zhang, Yin Li: design, data analysis, manuscript editing and manuscript review.

## REFERENCES

1. Kojima M, Hosoda H, Date Y, Nakazato M, Matsuo H, Kangawa K. Ghrelin is a growth-hormone-releasing acylated peptide from stomach. Nature 1999; 402: 656-60.
2. Asakawa A, Inui A, Kaga T, Yuzuriha H, Nagata T, Ueno N, *et al*. Ghrelin is an appetite-stimulatory signal from stomach with structural resemblance to motilin. Gastroenterology 2001; 120: 337-45.
3. Muccioli G, Tschöp M, Papotti M, Deghenghi R, Heiman M, Ghigo E. Neuroendocrine and peripheral activities of ghrelin: implications in metabolism and obesity. Eur J Pharmacol 2002; 440: 235-54.
4. Takachi K, Doki Y, Ishikawa O, Miyashiro I, Sasaki Y, Ohigashi H, *et al*. Postoperative ghrelin levels and delayed recovery from body weight loss after distal or total gastrectomy. J Surg Res 2006; 130: 1-7.
5. Doki Y, Takachi K, Ishikawa O, Miyashiro I, Sasaki Y, Ohigashi H, *et al*. Ghrelin reduction after esophageal substitution and its correlation to postoperative body weight loss in esophageal cancer patients. Surgery 2006; 139: 797-805.
6. Takiguchi S, Murakami K, Yanagimoto Y, Takata A, Miyazaki Y, Mori M, *et al*. Clinical application of ghrelin in the field of surgery. Surg Today 2015; 45: 801-7.
7. Delhanty PJ, Neggers SJ, van der Lely AJ. Mechanisms in endocrinology: Ghrelin: the differences between acyl- and des-acyl ghrelin. Eur J Endocrinol 2012; 167: 601-8.
8. Dordevic AL, Konstantopoulos N, Cameron-Smith D. 3T3-L1 preadipocytes exhibit heightened monocyte-chemoattractant protein-1 response to acute fatty acid exposure. PLoS One 2014; 9: e99382.
9. Meijer K, de Vries M, Al-Lahham S, Bruinenberg M, Weening D, Dijkstra M, *et al*. Human primary adipocytes exhibit immune cell function:

adipocytes prime inflammation independent of macrophages. PLoS One 2011; 6: e17154.
10. Osborn O, Olefsky JM. The cellular and signaling networks linking the immune system and metabolism in disease. Nat Med 2012; 18: 363-74.
11. Glass CK, Olefsky JM. Inflammation and lipid signaling in the etiology of insulin resistance. Cell Metab 2012; 15: 635-45.
12. Ide J, Gagnon A, Molgat AS, Landry A, Foster C, Sorisky A. Macrophage-conditioned medium inhibits the activation of cyclin-dependent kinase 2 by adipogenic inducers in 3T3-L1 preadipocytes. J Cell Physiol 2011; 226: 2297-306.
13. Harford KA, Reynolds CM, McGillicuddy FC, Roche HM. Fats, inflammation and insulin resistance: insights to the role of macrophage and T-cell accumulation in adipose tissue. Proc Nutr Soc 2011; 70: 408-17.
14. Amano SU, Cohen JL, Vangala P, Tencerova M, Nicoloro SM, Yawe JC, *et al*. Local proliferation of macrophages contributes to obesity-associated adipose tissue inflammation. Cell Metab 2014; 19: 162-71.
15. Sica A, Mantovani A. Macrophage plasticity and polarization: in vivo veritas. J Clin Invest 2012; 122: 787-95.
16. Mantovani A, Sica A. Macrophages, innate immunity and cancer: balance, tolerance, and diversity. Curr Opin Immunol 2010; 22: 231-7.
17. Xue N, Zhou Q, Ji M, Jin J, Lai F, Chen J, *et al*. Chlorogenic acid inhibits glioblastoma growth through repolarizating macrophage from M2 to M1 phenotype. Sci Rep 2017; 7: 39011.
18. Kotwal GJ, Chien S. Macrophage Differentiation in Normal and Accelerated Wound Healing. Results Probl Cell Differ 2017; 62: 353-64.
19. Chen S, Li R, Cheng C, Xu JY, Jin C, Gao F, *et al*. Pseudomonas aeruginosa infection alters the macrophage phenotype switching process during wound healing in diabetic mice. Cell Biol Int 2018; 42: 877-89.
20. Fujisaka S, Usui I, Bukhari A, Ikutani M, Oya T, Kanatani Y, *et al*. Regulatory mechanisms for adipose tissue M1 and M2 macrophages in diet-induced obese mice. Diabetes 2009; 58: 2574-82.
21. Lumeng CN, Bodzin JL, Saltiel AR. Obesity induces a phenotypic switch in adipose tissue macrophage polarization. J Clin Invest 2007; 117: 175-84.
22. Glass CK, Ogawa S. Combinatorial roles of nuclear receptors in inflammation and immunity. Nat Rev Immunol 2006; 6: 44-55.
23. Klotz L, Schmidt S, Heun R, Klockgether T, Kolsch H. Association of the PPARgamma gene polymorphism Pro12Ala with delayed onset of multiple sclerosis. Neurosci Lett 2009; 449: 81-3.
24. Regieli JJ, Jukema JW, Doevendans PA, Zwinderman AH, van der Graaf Y, Kastelein JJ, *et al*. PPAR gamma variant influences angiographic outcome and 10-year cardiovascular risk in male symptomatic coronary artery disease patients. Diabetes Care 2009; 32: 839-44.
25. Martin H. Role of PPAR-gamma in inflammation. Prospects for therapeutic intervention by food components. Mutat Res 2010; 690: 57-63.
26. Xu H, Barnes GT, Yang Q, Tan G, Yang D, Chou CJ, *et al*. Chronic inflammation in fat plays a crucial role in the development of obesity-related insulin resistance. Journal of Clinical Investigation 2003; 112: 1821-30.
27. Yamauchi T, Kamon J, Waki H, Murakami K, Motojima K, Komeda K, *et al*. The mechanisms by which both heterozygous peroxisome proliferator-activated receptor gamma (PPARgamma) deficiency and PPARgamma agonist improve insulin resistance. J Biol Chem 2001; 276: 41245-54.
28. Guri AJ, Hontecillas R, Ferrer G, Casagran O, Wankhade U, Noble AM, *et al*. Loss of PPAR gamma in immune cells impairs the ability of abscisic acid to improve insulin sensitivity by suppressing monocyte chemoattractant protein-1 expression and macrophage infiltration into white adipose tissue. J Nutr Biochem 2008; 19: 216-28.
29. Hevener AL, Olefsky JM, Reichart D, Nguyen MT, Bandyopadyhay G, Leung HY, *et al*. Macrophage PPAR gamma is required for normal skeletal muscle and hepatic insulin sensitivity and full antidiabetic effects of thiazolidinediones. J Clin Invest 2007; 117: 1658-69.
30. Marx N, Kehrle B, Kohlhammer K, Grüb M, Koenig W, Hombach V, *et al*. PPAR activators as antiinflammatory mediators in human T lymphocytes: implications for atherosclerosis and transplantation-associated arteriosclerosis. Circ Res 2002; 90: 703-10.
31. Xu G, Li Y, An W, Li S, Guan Y, Wang N, *et al*. Gastric mammalian target of rapamycin signaling regulates ghrelin production and food intake. Endocrinology 2009; 150: 3637-44.
32. Mossmann D, Park S, Hall MN. mTOR signalling and cellular metabolism are mutual determinants in cancer. Nat Rev Cancer 2018; 18: 744-57.
33. Saxton RA, Sabatini DM. mTOR Signaling in Growth, Metabolism, and Disease. Cell 2017; 169: 361-71.
34. Memmott RM, Dennis PA. Akt-dependent and -independent mechanisms of mTOR regulation in cancer. Cell Signal 2009; 21: 656-64.
35. Laplante M, Sabatini DM. mTOR signaling in growth control and disease. Cell 2012; 149: 274-93.
36. Gangoiti P, Arana L, Ouro A, Granado MH, Trueba M, Gomez-Munoz A. Activation of mTOR and RhoA is a major mechanism by which Ceramide 1-phosphate stimulates macrophage proliferation. Cell Signal 2011; 23: 27-34.
37. Vgontzas AN, Bixler EO, Papanicolaou DA, Chrousos GP. Chronic systemic inflammation in overweight and obese adults. Jama 2000; 283: 2235; author reply 6.
38. Van den Berghe G. How does blood glucose control with insulin save lives in intensive care? Journal of Clinical Investigation 2004; 114: 1187-95.
39. Cani PD, Amar J, Iglesias MA, Poggi M, Knauf C, Bastelica D, *et al*. Metabolic endotoxemia initiates obesity and insulin resistance. Diabetes 2007; 56: 1761-72.
40. Elbaz M, Gershon E. Ghrelin, via corticotropin-releasing factor receptors, reduces glucose uptake and increases lipid content in mouse myoblasts cells.Physiol Rep. 2021;9: e14654.
41. Perna S, Spadaccini D, Gasparri C, Peroni G, Infantino V, Iannello G, *et al*. Association between des-acyl ghrelin at fasting and predictive index of muscle derangement, metabolic markers and eating disorders: a cross-sectional study in overweight and obese adults. Nutr Neurosci. 2020;1-7. doi: 10.1080/1028415X.2020.1752997.
42. Cederberg H, Koivisto VM, Jokelainen J, Surcel HM, Keinanen-Kiukaanniemi S, Rajala U. Unacylated ghrelin is associated with changes in insulin sensitivity and lipid profile during an exercise intervention. Clin Endocrinol (Oxf) 2012; 76: 39-45.
43. Benso A, St-Pierre DH, Prodam F, Gramaglia E, Granata R, van der Lely AJ, *et al*. Metabolic effects of overnight continuous infusion of unacylated ghrelin in humans. Eur J Endocrinol 2012; 166: 911-6.
44. Sica A, Invernizzi P, Mantovani A. Macrophage plasticity and polarization in liver homeostasis and pathology. Hepatology 2014; 59: 2034-42.
45. Luo W, Xu Q, Wang Q, Wu H, Hua J. Effect of modulation of PPAR-gamma activity on Kupffer cells M1/M2 polarization in the development of non-alcoholic fatty liver disease. Sci Rep 2017; 7: 44612.
46. Patel L, Pass I, Coxon P, Downes CP, Smith SA, Macphee CH. Tumor suppressor and anti-inflammatory actions of PPARgamma agonists are mediated via upregulation of PTEN. Curr Biol 2001; 11: 764-8.
47. Marquard FE, Jucker M. PI3K/AKT/mTOR signaling as a molecular target in head and neck cancer. Biochem Pharmacol 2019: 113729.

**How to cite this article:** Yuan F, Zhang Q, Dong H, Xiang X, Zhang W, Zhang Y, *et al*. Effects of des-acyl ghrelin on insulin sensitivity and macrophage polarization in adipose tissue. J Transl Intern Med 2021; 9: 84-97.